

Development of the GPM Observatory Thermal Vacuum Test Model

Kan Yang and Hume Peabody

NASA Goddard Space Flight Center, Greenbelt, MD, 20771

ABSTRACT

A software-based thermal modeling process was documented for generating the thermal panel settings necessary to simulate worst-case on-orbit flight environments in an observatory-level thermal vacuum test setup. The method for creating such a thermal model involved four major steps: (1) determining the major thermal zones for test as indicated by the major dissipating components on the spacecraft, then mapping the major heat flows between these components; (2) finding the flight equivalent sink temperatures for these test thermal zones; (3) determining the thermal test ground support equipment (GSE) design and initial thermal panel settings based on the equivalent sink temperatures; and (4) adjusting the panel settings in the test model to match heat flows and temperatures with the flight model. The observatory test thermal model developed from this process allows quick predictions of the performance of the thermal vacuum test design.

In this work, the method described above was applied to the Global Precipitation Measurement (GPM) core observatory spacecraft, a joint project between NASA and the Japanese Aerospace Exploration Agency (JAXA) which is currently being integrated at NASA Goddard Space Flight Center for launch in Early 2014. From preliminary results, the thermal test model generated from this process shows that the heat flows and temperatures match fairly well with the flight thermal model, indicating that the test model can simulate fairly accurately the conditions on-orbit. However, further analysis is needed to determine the best test configuration possible to validate the GPM thermal design before the start of environmental testing later this year. Also, while this analysis method has been applied solely to GPM, it should be emphasized that the same process can be applied to any mission to develop an effective test setup and panel settings which accurately simulate on-orbit thermal environments.

INTRODUCTION

The Global Precipitation Measurement (GPM) mission is a satellite constellation developed in conjunction with various international partners to provide next-generation global observations of precipitation and climate change. The GPM core observatory satellite, developed by NASA and the Japanese Aerospace Exploration Agency (JAXA), carries an advanced radar/radiometer system and serves as a reference standard to unify all of the measurements from the GPM constellation. The scientific data gained from the core observatory and the larger constellation will help advance the current understanding of the water and energy cycle, improve forecasting of extreme weather events, and extend existing capabilities to use precipitation information to benefit society.

The major components of the GPM core observatory spacecraft, as well as the manufacturers for each component, are shown in Figure 1. The spacecraft bus is developed and integrated at NASA Goddard Space Flight Center (GSFC) and consists of three components: a Lower Bus Structure centrally located on the spacecraft; an Avionics Module (AM) in the $-Z$ direction of the LBS, and an Upper Bus Structure (UBS) in the $+X$ direction of the LBS, as per the axes defined in the figure. The LBS contains the drive assemblies for the solar arrays as well as attachments for the solar array booms, the reaction wheels, and the GPS boxes. The propulsion system is enclosed within the LBS and occupies the aft end ($-X$) of the spacecraft. The AM contains most of the avionics boxes as well as the batteries and star trackers. The UBS contains the RF boxes as well as the High-Gain Antenna System (HGAS). Two instruments complete the spacecraft assembly: the GPM Microwave Imager (GMI), developed by Ball Aerospace Corporation; and the Dual Precipitation Radars (DPR), built by JAXA, which include the Ka-Band and Ku-Band Precipitation Radars (KaPR and KuPR).

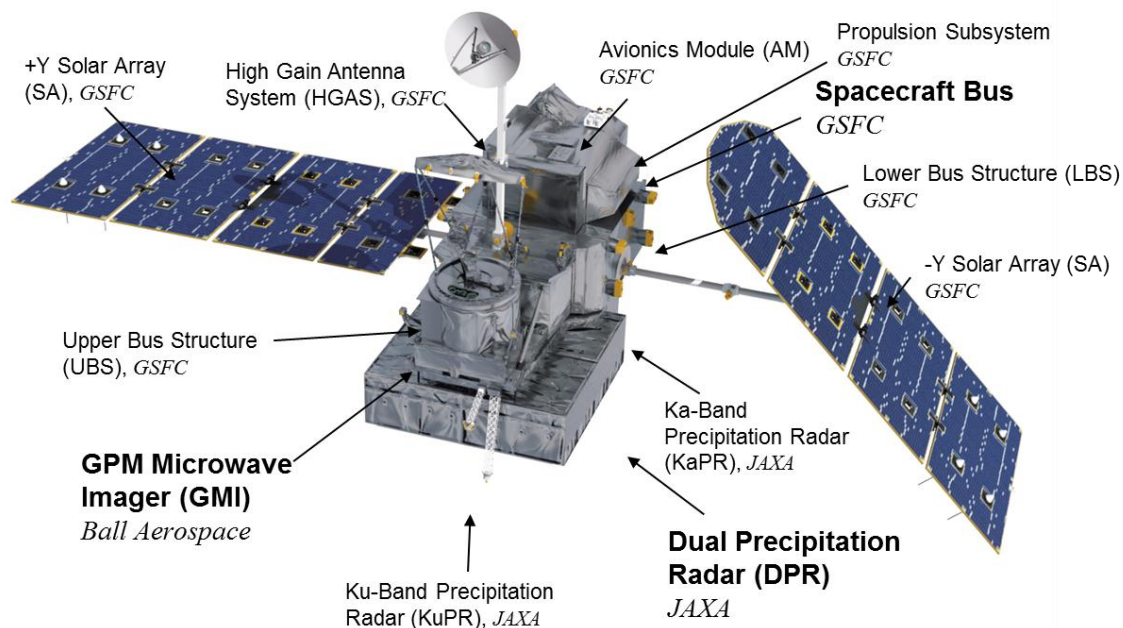


Figure 1. Major Components of the GPM Spacecraft.

GPM is scheduled to launch from Japan in early 2014. Before launch, GPM must undergo environmental testing, notably thermal testing, to verify that the spacecraft works in its intended mission environment. To this end, the test environment must be able to accurately simulate the worst case environments on-orbit. By simulating the worst-case conditions, one can verify that the thermal design of the spacecraft works, that the thermal model of the spacecraft gives accurate predictions, and that all hardware components will be able to survive the range of expected flight conditions. However, the design of the test environment as well as the settings for the thermal hardware must be first determined via modeling, such that a programmatically feasible design can be achieved. The ultimate goal of the thermal test design is to be capable of simulating all of the worst flight environments, as well as to match as close as possible all of the flight heat flows and temperatures across the spacecraft.

Through the methodology documented in this work, a “test thermal model” is developed which incorporates the flight observatory model plus thermal test ground support equipment (GSE), including thermal test panels which can be used to simulate flight sink temperatures and environments. This test model can predict the performance of the thermal test setup before any test hardware is built. In addition, while the heat flows and temperatures predicted for this work relate specifically to the GPM project, this methodology can be used directly with any low-Earth orbiting mission, or can be extended to encompass any spacecraft mission

THERMAL ANALYSIS METHOD

The analysis method to design a thermal test which can accurately simulate flight environments is four-fold, and includes the following steps: (1) determining the major thermal zones for test as indicated by the major dissipating components on the spacecraft, then mapping the major heat flows between these components. (2) finding the flight equivalent sink temperatures for these test thermal zones; (3) determining the thermal test ground support equipment (GSE) design and initial thermal panel settings based on the equivalent sink temperatures; and (4) adjusting the panel settings in the test model to match heat flows and temperatures with the flight model. Steps (2) and (4) are not design-specific and hence are discussed first. Steps (1) and (3) are specific to GPM and will be discussed afterward.

Equivalent Sink Temperatures

To simulate an on-orbit environment with ground testing, the test GSE must be able to replicate the environmental sources and other conditions that the spacecraft sees in flight. These include multiple environmental sources as well as backloading, i.e. the energy exchanges from one surface to another on the spacecraft. As shown in Figure 2, for any given radiating surface on the spacecraft, that surface sees environmental loading from solar energy, Q_{solar} ; albedo, Q_{Albedo} ; and Earth infrared energy, $Q_{Earth\ IR}$. The surface is also radiating heat to space, $Q_{Out,Space}$, and is exchanging heat with other surfaces on the spacecraft, $Q_{Backload}$.

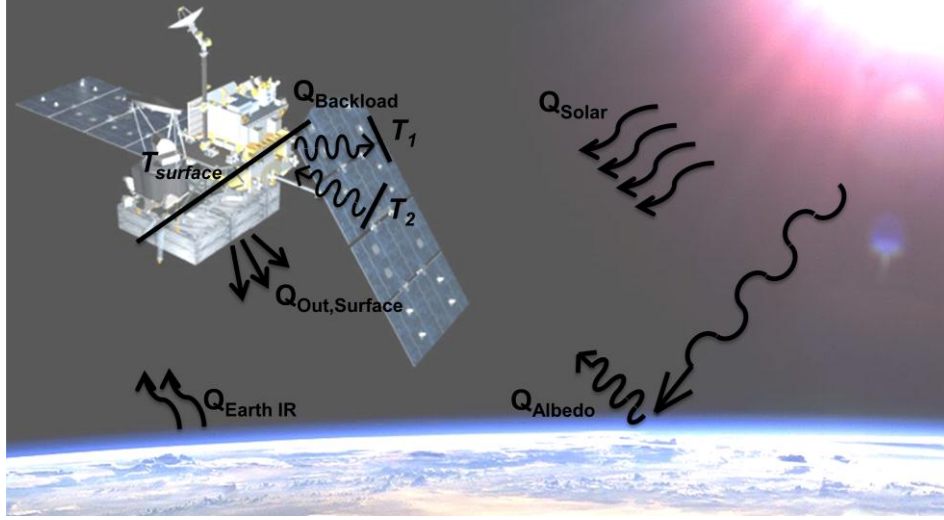


Figure 2. Typical Heat Exchanges for Low-Earth Orbits.

In an ideal thermal test, all of these heat sources would be included to generate the best-possible flight-like environment. However, due to logistical and programmatic restrictions for thermal testing, not all of these environmental factors can be simulated. Therefore, a substitute IR source which consists of a thermal panel set at an equivalent sink temperature is used to mimic the effects of these sources.

The equivalent sink temperature for any surface on the spacecraft, as explained by Peabody [1] and Juhasz [2], is an “equilibrium” temperature reached by a passively radiating surface from exchanging thermal radiation energy with the space environment and with other spacecraft components visible to that surface. It varies as a function of distance to the sun, beta angle between the spacecraft’s orbit plane and the solar vector, and the optical characteristics of the radiating surface. By mathematically equating the energy balance of the spacecraft in flight with the energy balance of the test spacecraft incorporating an IR source at a sink temperature, one arrives at the following equation:

$$Q_{solar} + Q_{albedo} + Q_{EarthIR} + (Q_{backload} - Q_{Out, Surface}) = Q_{Sink} - Q_{Out, Surface} \quad \text{Eq. 1}$$

Q_{env} can represent the first three terms in the equation. $Q_{backload}$ is the heat lost or gained between a given surface, i , and all other surfaces j within its field of view; it can be expressed as

$Q_{backload} = \sigma \sum_j^{1,N} Radk_{ij} T_j^4$. The final term, $Q_{Out, surface}$, represents the radiative rejection of heat from

the surface i . On the right-hand side of the equation, Q_{sink} can be expressed for a particular surface as $Q_{i, Sink} = \sigma \sum_j^{1,N} Radk_{ij} T_{i, Sink}^4$. Thus, Eq.1 can be written as:

$$Q_{env} + \sigma \sum_j^{1,N} Radk_{ij} T_j^4 - \sigma \sum_j^{1,N} Radk_{ij} T_i^4 = \sigma \sum_j^{1,N} Radk_{ij} (T_{i, Sink}^4 - T_i^4) \quad \text{Eq. 2}$$

Where

$$Radk_{ij} = A_i \varepsilon_i B_{ij} \quad \text{Eq. 3}$$

$Radk_{ij}$ represents the radiative coupling between surface i and surface j , expressed as the product of the area and emissivity of surface i with the energy exchange factor B_{ij} between the two surfaces. By rearranging Eq. 2 to solve for $T_{i,Sink}$, we have:

$$T_{i,Sink}^4 = \frac{\sigma \sum_j^{1,N} Radk_{ij} T_j^4 + Q_{env}}{\sigma \sum_j^{1,N} Radk_{ij}} \quad \text{Eq. 4}$$

Furthermore, since test thermal panels are not perfect sinks, i.e. it is not feasible to create a panel with $\varepsilon = 1$, this effect must be accounted for in the sink temperature calculation. Therefore, the final sink temperature for the replacement source is estimated by the equation:

$$T_{i,imperfect} \approx \left\{ \left[T_{i,Sink}^4 + (\varepsilon - 1)T_i^4 \right] / \varepsilon \right\}^{1/4} \quad \text{Eq. 5}$$

The sink temperature is calculated using this method for every node, i.e. calculation point, within the thermal model.

Since it is not programmatically feasible to set every thermal node to its own respective sink temperature within the test setup, from the previous sink temperature calculations, nodes with similar sink temperatures or nodes which reside in the same major radiating surface on the spacecraft will be grouped into a thermal zone. All nodes in a particular thermal zone will view its zone-dedicated thermal panel set at the appropriate sink temperature. However, in this zone there will still be temporal and spatial variations in sink temperature. In response, a “composite” or weighted sink temperature must be utilized such that a single sink temperature setting can be determined for an entire thermal zone. This equation is presented as follows:

$$T_{Sink,Weighted}^4 = \frac{\sum_i^{1,N} (RadkSum_i T_i^4)}{\sum_i^{1,N} RadkSum_i} \quad \text{Eq. 6}$$

Equation 6 allows a final, composite sink temperature to be calculated that weights higher the high emissivity and large area surfaces, and weights lower the low emissivity and smaller area surfaces. The T^4 term also puts more weight on high-temperature surfaces. For all major radiating surfaces on the spacecraft, this process is used to establish the sink temperatures per thermal zone for the worst-case hot and cold environmental scenarios; Gilmore [3] presents typical parameters for worst-case scenarios. However, it must be emphasized again that these composite sink temperatures are compromises due to the limitations of the test setup; it is not the ideal sink temperature for every node in that zone. Hence, the heat flows and temperatures achieved on the test setup will not match exactly with flight values, but rather achieve a “closest possible” despite test setup restrictions.

Iterative Design and Analysis with the Test Thermal Model

A test model was generated by modifying the existing Thermal Desktop [4] software-based spacecraft observatory thermal model by removing all components not present in the observatory test, then adding thermal GSE to simulate its configuration inside the test chamber. Upon completion of a preliminary thermal test model, Figure 3 shows the iterative process for obtaining “finalized” preliminary temperature setpoints for the panels.

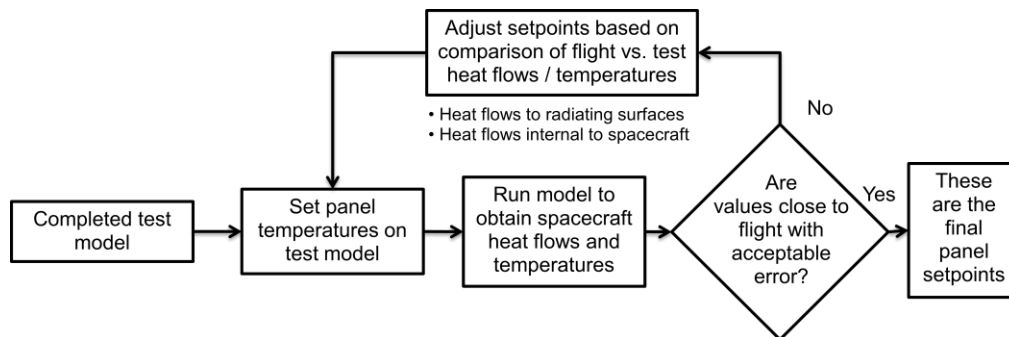


Figure 3. Iterative process for obtaining “finalized” preliminary panel setpoints using the observatory thermal test model.

The completed test model first has its panels set to the initial sink temperatures calculated from the process presented above. It is then solved using the Systems Integrated Numerical Differencing Analyzer (SINDA) [5] thermal analysis suite with the current panel settings. From the results, one can deduce major heat flows between components and temperatures on the components. For the purpose of comparing the accuracy of the test model at simulating the flight model’s environment, major heat flows between internal components and radiating surfaces were examined. The amount of heat flowing between these two areas of the spacecraft is established by grouping all of the environment-viewing nodes on the radiating surface in one control volume, and all of the internal nodes that are conductively coupled to the radiating surface in another control volume, then determining the amount of heat flowing between the two control volumes via the model results. After obtaining the heat flows and temperatures, a decision must be made if the test model values are close enough to the flight values with an acceptable error. A good match of heat flows and temperatures implies that the test model correlates well with the flight model, and therefore that the test model is fairly accurately predicting the on-orbit flight environment. It was decided that an “acceptable error” implies that the heat flows from internal component to radiating surface per zone were within 10% of the flight values, and the component temperatures matched to within $\pm 5^{\circ}\text{C}$ of their flight values. If the heat flows and temperatures did not correspond well, new panel sink temperature setpoints were determined for the next iteration of the model. This was accomplished by deducing if the sink temperatures needed to be colder or hotter based on the heat flow and temperatures of the zone in the test model in relation to the flight model. Once the panels were reset, the model could be rerun to obtain new heat flows and temperatures; if the values matched to the flight values with acceptable error, the current panel settings would become the final setpoints.

Further design considerations were incorporated into the thermal test setup, including incorporating the requirements of other subsystems. Thermal panels were placed as close as

possible to the radiating surfaces in their dedicated zones such that most of the view of the radiators would be covered by the test panel. Test blanketing was used to restrict the view of a radiating surface to its specific test panel and to prevent views from components in one zone to panels in another zone – a practice known as “blanket tunneling.” The concerns of other subsystems, particularly with the mechanical feasibility of a thermal test panel design as well as the need for contamination monitors and harness entry points, also resulted in concessions with the thermal design. Finally, hardware selection for thermal panels factored into the analysis: cryopanel, which require a constant liquid or gaseous nitrogen feed line to control temperatures, were placed where heat flows from the radiating surface were large; heater panels, which heat via heaters and cool solely via passive radiation, were placed where heat flows to the panel were small and slower cooling rates were acceptable.

Heat flows on the GPM Spacecraft

For the GPM observatory thermal vacuum test, the number of thermal zones on the spacecraft was determined by the number and location of major radiating surfaces on the observatory, as shown in Figure 4. As mentioned in the previous section, thermal panels were placed facing these radiative surfaces such that the panel setpoints allow control of the heat flows from the spacecraft and temperature of components on the spacecraft. It should be noted that although the solar panels are not present in the thermal vacuum test assembly due to space restrictions, the effect of the solar arrays is included in the sink temperature calculations since they were obtained from the flight configuration of the spacecraft.

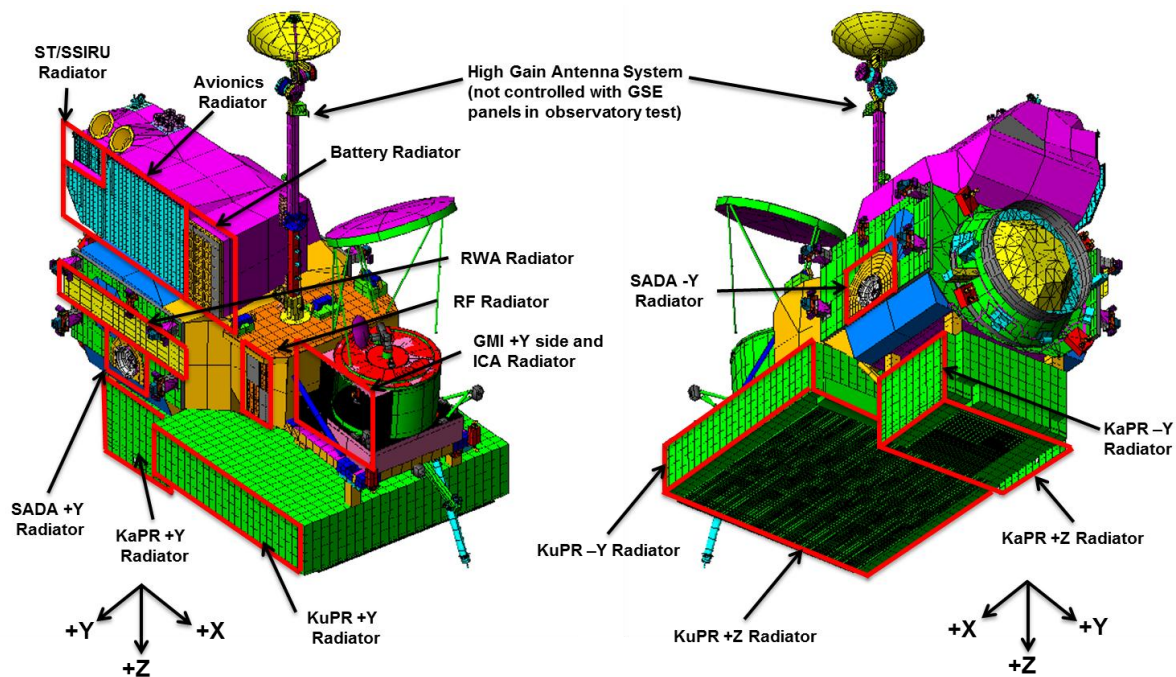


Figure 4. Major Radiating Surfaces on GPM.

Deducing from the number of major radiating surfaces on the spacecraft, there are a total of sixteen zones that are required for large-scale control of the spacecraft heat flows and temperatures. The first zone comprises the Avionics Radiator, Battery Radiator, and Star Tracker/Space Scalable Inertial Reference Unit (ST/SSIRU) Radiator; other zones are for the Reaction Wheel Assembly (RWA) radiator, the +Y and -Y Solar Array Drive Assembly (SADA) radiators, the GMI +Y radiators, the RF radiator, radiating surfaces on the propulsion component assembly and propulsion tanks, the KaPR and KuPR +Y, -Y, and +Z radiators. For each zone, in addition to the environmental sources, internal components conduct or radiate heat to the major radiative surfaces in that zone. Understanding the heat flows between components and radiating surfaces in each zone is crucial to comprehending how waste heat is dissipated from the interior of the spacecraft via the radiator, and out to space. Therefore, if the heat flows match between the test model and flight model, the test model's ability to simulate flight-like conditions can be verified.

As an example, this work will presently focus on the heat paths through the avionics module (AM) zone, which comprise the heat rejected by the avionics, battery, and ST/SSIRU radiators. However, the reader shall understand that the avionics module heat flows presented here are an analogy for heat flows in all the thermal zones on the spacecraft. Figure 5 shows the major component heat paths in the AM zone. The lines in the figure are defined by the paths taken by the heat generated from avionics components to a radiating surface. Specifically in the AM, there are three major radiating surfaces: the ST/SSIRU Radiator, the Avionics Radiator, and the Battery Radiator. For the ST/SSIRU assembly, the Star Trackers and SSIRU conductively dissipate heat through the Shelf. The Star Tracker Heat Pipes are mounted with Nusil, a thermally conductive interface material, to the Shelf and the ST/SSIRU Radiator, and allow transport of heat from one component to the other. When the heat reaches the radiator, it is rejected out to the environment. The Avionics boxes, namely the Power System Electronics (PSE), the Propulsion Interface Electronics (PIE), the GPS tower, the Mechanism Attitude and Control Electronics (MACE), and the Command and Data Handling (C&DH) boxes, are bolted with Nusil for thermal conductivity and a copper frame for electrical grounding. They reject heat to the avionics module structure, which has four avionics heat pipes to transport heat to the Avionics Radiator. The radiator then rejects heat to space. The battery assembly has the batteries mounted with Cho-Therm, another type of thermal interface material, to the Battery Baseplate. Four Battery Heat Pipes then transport heat to the Battery Radiator, where it is then rejected to space. Though the Shelf, Avionics Module, and Battery Baseplate are all physically attached to each other, the interfaces between these components are isolated using thermal isolators and hence do not represent significant heat paths. Furthermore, the dashed lines in Figure 5 represent major heat flow paths between the internal components and space-viewing surfaces (i.e. the radiators). Again, it must be emphasized that the heat paths presented are representative of those for other zones; all other subsystems and instruments on the spacecraft have similar methods of rejecting heat to space: either through conductive heat paths and heat pipes to a radiator, or directly through a space-viewing surface on the component. Once all of the heat flows are captured, the values from the test model (along with temperatures of the components) can be matched against flight model values for accuracy.

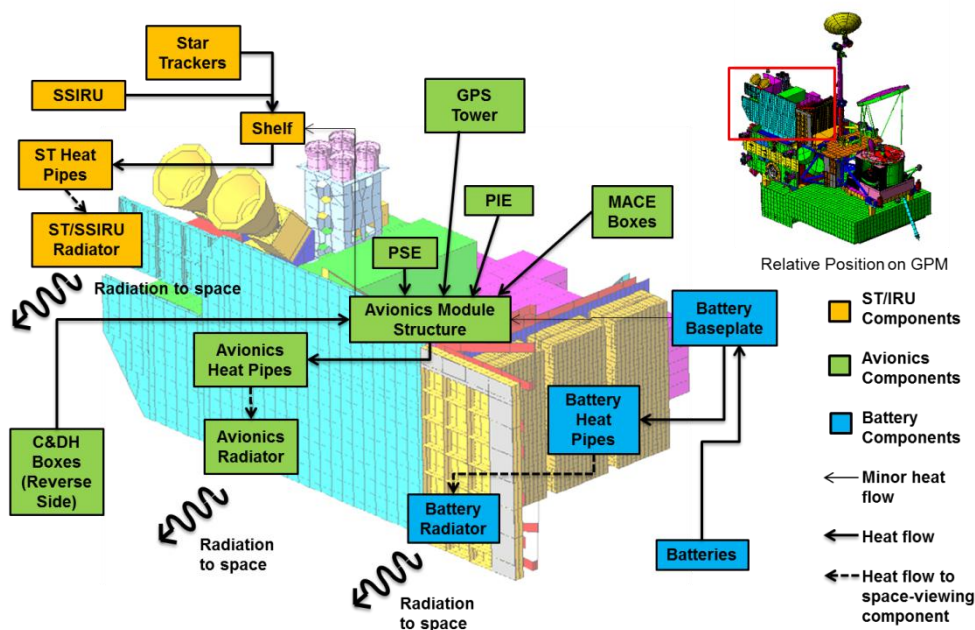


Figure 5. Major component heat paths in the GPM Avionics Module thermal zone.

THE GPM TEST THERMAL MODEL: DESIGN, ANALYSIS, AND RESULTS

The GPM observatory test thermal model was developed taking into account all the considerations presented thus far. The finalized model is shown in Figure 6. All of the zones with significant radiating surfaces view thermal GSE panels; test Multi-Layer Insulation (MLI) with a vapor-deposited aluminum (VDA) outer layer form blanket tunnels from the spacecraft to the panels where the blanketing is exposed to the shroud, while single-layer VDA is used for closeout between zones when the blanketing is not exposed to the shroud. Several design decisions should be noted: the $-Z$ side of the AM does not view any thermal panels since the correct heat flows were only achieved when the $-Z$ AM blanket viewed a cold test chamber wall. A cutout was made in the blanketing at the top end of the GMI fixture supporting the cryopanel since the blanketing interfered with the envelope in which the HGAS could rotate. Furthermore, the HGAS does not have heater panels since they were mechanically challenging to implement above the HGAS deck. Since the HGAS was already qualified during system-level testing, it was decided that during observatory-level testing that it will just radiate to the cold shroud, with test and flight heaters to control temperatures. In addition, a cutout was made in the SADA $+Y$ and $-Y$ panels to allow for the mounting of an electrical GSE fixture to simulate harness heating from the solar arrays.

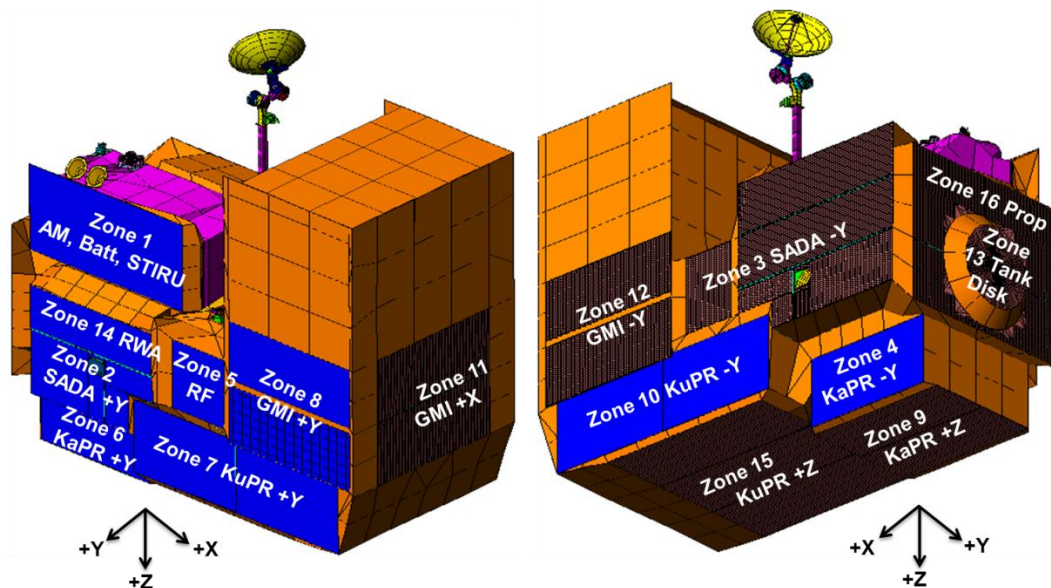


Figure 6. The GPM Observatory Test Model.

Table 1. Sink Temperatures and Panel Setpoints for worst-case hot and cold environments

Zone Number	Description	Cold Beta 90° (Temps in °C)		Hot Beta 0° (Temps in °C)	
		Sink Temperatures	Panel Setpoints	Sink Temperatures	Panel Setpoints
1	Avionics Radiator ST/SSIRU Radiator Battery Radiator	-127 -137 -124	-120	-90 -88 -88	-85
2	SADA +Y	-98	-60	-73	-50
3	SADA -Y	-42	-50	-35	-35
4	KaPR -Y	-62	-55	-34	-34
5	RF	-101	-70	-68	-55
6	KaPR +Y	-78	-70	-37	-37
7	KuPR +Y	-84	-80	-56	-56
8	GMI +Y GMI ICA Radiator	-86 -99	-100	-58 -79	-70
9	KaPR +Z	-35	-40	14	-10
10	KuPR -Y	-33	-35	-42	-50
11	GMI +X	-98	-70	-57	-40
12	GMI -Y	-21	-15	-78	-60
14	RWA Radiator	-98	-120	-60	-70
15	KuPR +Z	-35	-50	4	0

Using the iterative design and analysis method presented above, the initial panel setpoints were found by calculating the orbit-averaged sink temperature per zone using the Thermal Analysis Results Processor (TARP) [6] program, which employs the equivalent sink temperature equations on the flight model. The results were then verified via hand calculations and other independent methods. Then, the panel setpoints were iterated through the process until the final setpoints which best matched heat flows and temperatures were determined. The results for sink temperature on the spacecraft are presented in Table 1 for the worst-case hot environment, Hot

Beta 0°, and worst-case cold environment, Cold Beta 90°, that GPM encounters. These are also compared with the final panel setpoints. Since there aren't many significant radiating surfaces for the propulsion and tank disk zones because they are almost completely blanketed, their sink temperatures could not be calculated.

Table 2. Heat flow and temperature comparisons between test and flight models over all thermal zones for the Cold Beta 90 case

Zone Number	Description	Panel Setpoint (°C)	Heat Flows to Radiating Surface (W)			Temperatures (°C)		
			Test	Flight	$\Delta(Q_{\text{flight}} - Q_{\text{test}})$	Test	Flight	$\Delta(T_{\text{flight}} - T_{\text{test}})$
Zone 1 (Cryopanel)	AM Radiator	-120	259.6	255.8	-3.7	-9.7	-10.5	-0.8
	ST/SSIRU Radiator		34.4	33.9	-0.5	-7.9	-9.7	-1.8
	Battery Radiator		91.7	91.7	0	10.2	10.3	0.2
Zone 2 (Cryopanel)	SADA +Y Radiator	-60	15.9	18.3	2.3	0.6	0	-0.6
Zone 3 (Heater Panel)	SADA -Y Radiator	-50	30.4	26	-4.4	-5.2	-3	2.2
Zone 4 (Cryopanel)	KAPR -Y	-55	45.1	42.6	-2.4	-7	-7.5	-0.5
Zone 5 (Cryopanel)	RF Radiator	-70	36.7	40.1	3.4	8.8	7.2	-1.6
Zone 6 (Cryopanel)	KAPR +Y	-70	71.9	69.6	-2.3	-9.2	-9.7	-0.5
Zone 7 (Cryopanel)	KUPR +Y	-80	32.3	35	2.6	-42	-41.5	0.4
Zone 8 (Cryopanel)	GMI +Y	-100	10	10.7	0.7	-8.1	-7.4	0.6
	GMI ICA Radiator		28.7	28.8	0.1	11.8	11.7	-0.1
Zone 9 (Heater Panel)	KAPR +Z	-40	41.2	39.3	-1.9	-20	-19.9	0
Zone 10 (Cryopanel)	KUPR -Y	-35	13.5	13.9	0.4	-23	-17.2	5.6
Zone 11 (Heater Panel)	GMI +X	-70	-1.3	-1.1	0.2	-30	-33.7	-3.8
Zone 12 (Heater Panel)	GMI -Y	-15	-0.3	-0.4	-0.1	-12	-7.3	-4.2
Zone 13 (Heater Panel)	Tank Disk	-100	N/A	N/A	N/A	4.9	3.5	-1.4
Zone 14 (Cryopanel)	RWA Radiator	-120	96.9	94.6	-2.3	-11	-11.2	0
Zone 15 (Heater Panel)	KUPR +Z	-50	207.9	205.2	-2.7	-21	-13.5	7.3
Zone 16 (Heater Panel)	Propulsion	-100	N/A	N/A	N/A	7.8	6.4	-1.4

Table 3. Heat flow and temperature comparisons between test and flight models over all thermal zones for Hot Beta 0 case

Zone Number	Description	Panel Setpoint (°C)	Heat Flows to Radiating Surface (W)			Temperatures (°C)		
			Test	Flight	$\Delta(Q_{\text{flight}} - Q_{\text{test}})$	Test	Flight	$\Delta(T_{\text{flight}} - T_{\text{test}})$
Zone 1 (Cryopanel)	AM Radiator	-85	291.2	306.2	14.9	5.7	12.2	6.4
	ST/SSIRU Radiator		37.7	43.3	5.7	6.3	18.1	11.8
	Battery Radiator		83.4	72.9	-10.5	13.3	13.4	0.1
Zone 2 (Cryopanel)	SADA +Y Radiator	-50	14.7	17.2	2.5	4.9	5.8	1
Zone 3 (Heater Panel)	SADA -Y Radiator	-35	28.1	28.4	0.3	-0.6	-0.2	0.4
Zone 4 (Cryopanel)	KAPR -Y	-34	90.5	91.9	1.4	19.6	17.3	-2.3
Zone 5 (Cryopanel)	RF Radiator	-55	42	47.5	5.5	22.2	28.6	6.3
Zone 6 (Cryopanel)	KAPR +Y	-37	88.3	92	3.8	16.7	14	-2.6
Zone 7 (Cryopanel)	KUPR +Y	-56	50.9	49	-1.9	-15	-17.4	-2.9
Zone 8 (Cryopanel)	GMI +Y	-70	10.8	11.6	0.7	-2.1	0.3	2.4
	GMI ICA Radiator		29.4	33.3	3.9	22.3	20.9	-1.3
Zone 9 (Heater Panel)	KAPR +Z	-10	63.3	55.3	-8	10.6	10.8	0.1
Zone 10 (Cryopanel)	KUPR -Y	-50	37.8	36.7	-1	-15	-17.9	-3.4
Zone 11 (Heater Panel)	GMI +X	-40	-1.4	-1.1	0.3	-19	-20	-1
Zone 12 (Heater Panel)	GMI -Y	-60	-0.5	-0.4	0	-24	-26.3	-2
Zone 13 (Heater Panel)	Stub Skirt	-25	N/A	N/A	N/A	14.9	20.9	6
Zone 14 (Cryopanel)	RWA Radiator	-70	83	91.5	8.4	-2.4	7.1	9.5
Zone 15 (Heater Panel)	KUPR +Z	0	182.6	193	10.4	14.8	11.5	-3.3
Zone 16 (Heater Panel)	Propulsion	-30	N/A	N/A	N/A	15.8	20.9	5.1

The sink temperatures calculated from the flight model and panel settings were generally comparable, with a few discrepancies. Zones 2 and 14, which represent the SADA +Y and RWA Radiator zones, both have a sink temperature of -98°C in the cold case since they are physically adjacent to each other on the spacecraft and therefore are subject to very similar environments. However, the panel settings in test differ by 60°C in the cold case since the heat flows could not be matched with flight values unless there was a large temperature discrepancy. This is most likely due to the amount of spurious heat exchanged (“cross-talk”) between the two zones.

Though a test blanket does separate the two zones, there is still a significant amount of heat leak between them. Similar scenarios result in the discrepancies between the panel setpoints and sink temperatures in Zone 5 for the cold case and Zone 9 for the hot case; due to highly reflective VDA closeout blanketing as well as heat being reflected back onto the radiator from the panels (since the panels are not perfect emitters), the panel setpoints tend to be higher in temperature than the flight sink temperatures. Furthermore, since the GMI +X, GMI -Y, Propulsion, and Tank Disk zones were mostly flight-blanketed and the heat flow is small, only the temperatures were compared between the test and flight models to determine the appropriate panel settings.

The heat flows to the radiating surface obtained from the test model using “finalized” preliminary setpoints, as compared with the values from the flight model, are shown in tures could not be calculated.

Table 2 for a Cold Beta 90° case and Table 3 for a Hot Beta 0° case. Both tables show that the heat flow and temperature values from the test and flight models are comparable. For the Cold Beta 90° case, all of the test values are reasonably lie within the range of the orbit-averaged heat flows and temperatures encountered during flight. However, with Hot Beta 0°, since the sink temperatures fluctuate greatly over the course of the orbit, it was more difficult to match the flight and test values. Despite this, most of the test values for heat flow are within 15% of the flight value. For Zone 1, the discrepancies between flight and test heat flows are due to the compromise of grouping all the avionics module radiators in one thermal zone. For Zone 15, it was found that the +Z radiator on the KuPR was very sensitive to changes in heat source, and that small changes in the sink temperature equated to large changes in the heat flow from the +Z radiator out to the test panel. For example, if the +Z KuPR thermal panel raises slightly in temperature, less heat is rejected out of the +Z KuPR radiator and instead diverted to the KuPR +Y and -Y radiators. Therefore, it proved difficult with the iterative process to determine the accurate KuPR +Z panel settings, which caused the discrepancies between test and flight values for Zone 15.

With all factors taken into consideration, the overall test and flight heat flows matched well, indicating that the test model is fairly accurate in simulating the worst-case environments on orbit. It should be noted, though, that not all of the values of heat flow and temperature from the test model match the flight model within the “acceptable error” as defined earlier. Due to the complexity of the test design, the imperfect substitute of IR panels for all of the heat sources in the flight environment, and the temporal and spatial averaging of sink temperatures, only the “best case scenario” with the current analysis could be achieved. Further refinements to the analysis need to be undertaken to capture all of the myriad factors that influence the test to arrive at more refined sink temperatures, taking into consideration that the final temperature setpoints during the test may not be achievable until the actual observatory is undergoing thermal vacuum testing.

CONCLUSIONS

This work developed and documented a process by which the thermal observatory test design could be generated for any low-Earth orbiting spacecraft. The four steps for determining the

thermal panel settings for the observatory test were chronicled as follows: (1) identifying the major thermal zones and mapping the major heat flows; (2) finding the flight equivalent sink temperatures for each zone; (3) determining the thermal test model design and initial panel settings; and (4) adjusting the panel settings using an iterative process to match test model heat flows and temperatures with flight. This process was applied to the observatory thermal vacuum test design of the GPM project.

For GPM, the preliminary thermal observatory test GSE design was documented and the “finalized” preliminary thermal panel settings from the model were determined. With the current panel settings, the analysis results showed that the test model produces heat flows and temperatures that agree fairly accurately with the flight values. This indicates that the test setup is successful in simulating the worst-case environments seen during flight. However, certain thermal zones such as the KuPR and Avionics Module in the worst case hot conditions showed values where flight and test didn’t agree as well, and these are mostly representative of the compromises in the thermal design to create a logistically and programmatically feasible test. In addition, although the test design for GPM has been generated, allowing for the fabrication for thermal panels and other test GSE, the panel settings have only been “finalized”, but are not “final”. In an actual observatory-level test, conditions will always vary somewhat from the model, and as such panel setpoints will change. However, the current design of the test setup is versatile enough where changes can be made to the thermal panel settings to allow the sink temperatures to change without requiring a change of the hardware.

REFERENCES

1. Peabody, Hume. “Backloads and Equivalent Sinks.” *TARP v3.1: Thermal Analysis Results Processor Manual*. Feb., 2009.
2. Juhasz, Albert J. “An Analysis and Procedure for Determining Space Environmental Sink Temperatures With Selected Computational Results” NASA Technical Memorandum TM-2001-210063. NASA Glenn Research Center, Cleveland, OH. 2001.
3. Gilmore, David G. et al. “Thermal.” *Space Mission Analysis and Design*. Ed. James R. Wertz and Wiley J. Larson. 3rd Edition. Hawthorne, CA: Microcosm Press, 1999.
4. Cullimore and Ring Technologies. *Thermal Desktop*. Version 5.4, 2011. Computer Program.
5. Cullimore and Ring Technologies. *SINDA/FLUINT*. Version 5.4, 2011. Computer Program.
6. Thermal Modeling Solutions, LLC. *TARP: Thermal Analysis Results Processor*. Version 4.0.14. 2012. Computer Program.